#24-088
2024 AFS Proceedings ©American Foundry Society

Effects of Silicon in High-Cr White Cast Irons

Richard B. Gundlach
Gundlach Consulting Services, Farmington, Michigan, USA

John M Tartaglia
Element Materials Technology, Wixom, Michigan, USA

ABSTRACT

This research characterized the effects of Si on eutectic saturation, the ideal hardening temperature, hardenability, carbide fraction, and alloying element content in the constituents of high-Cr white cast irons to improve performance. Hypoeutectic alloys of 15% and 25% Cr white irons were produced with Si levels varying of 0.4%, 1% and 1.6%Si and poured into 3-inch (75-mm) Y-block sand molds.

Various tests were used to determine the optimum hardening temperature and the kinetics of pearlite transformation. In addition, image analysis was performed to determine eutectic carbide fraction. Furthermore, scanning electron microscopy/energy dispersive spectroscopy (SEM/EDS) analysis was conducted to determine the distributions of the alloying elements among the various solidification constituents.

Raising Cr from 15% to 25% caused the optimum hardening temperature to rise from 1680 to 1920F (915 to 1050C). In the 15% Cr series, an increase of 1.2% Si raised the optimum hardening temperature by 80F (50C), whereas, for the 25% Cr series, the optimum hardening temperature was unchanged.

Peak hardness was significantly higher (by 50 HB) in the leaner Cr alloys and the peak hardness in both the 15% and 25% Cr alloys decreased slightly (by 20 HB) when the Si content was increased from 0.4% to 1.6%. However, the hardenability (the time to the onset of pearlite transformation) increased with increasing Si content.

The influence of Si on % eutectic saturation was not clear. When analyzing carbide fraction, Si had a negligible effect in the 15% Cr series, but seemed to cause the 25% Cr series to develop less eutectic carbide, that is, become more hypoeutectic. The Cr was richest in the eutectic carbides and leanest in the eutectic austenite matrix. The Si was largely rejected from the eutectic carbides and richest in the eutectic austenite.

Keywords: white cast iron, chromium, silicon, heat treatment, hardenability, austenite destabilization

INTRODUCTION

High-chromium white cast irons (HCWI) have excellent abrasion resistance and are used effectively in brick molds, coal-grinding mills, shot-blasting equipment, slurry pumps, and components for quarrying, hard-rock mining, and milling. In some applications they must also withstand heavy impact loading. These alloyed white irons are recognized as providing the best combination of toughness and abrasion resistance attainable among the white cast irons family.

As a class of alloyed irons, the HCWI are distinguished by the hard, and relatively discontinuous M_7C_3 eutectic Cr carbides present in the microstructure, as opposed to the softer, more continuous M_3C eutectic carbides present in the Ni-Cr white irons containing less chromium. For most applications, the HCWI castings are heat treated to produce a hard martensitic matrix.

Silicon is a common alloying element that cannot be avoided in HCWI. The high C and Cr concentrations make it unnecessary to deoxidize heats of HCWI alloys, and Si is often considered a tramp element incorporated from various charge materials and from high-carbon ferrochromium additions, some of which often contain quite high Si concentrations. ASTM specification A532 generally restricts Si to a maximum of 1.5%.[1] Nevertheless, Si has unique attributes that influence the microstructure and hardenability of heat-treated castings.

Among the diverse characteristics reported for Si are the following:

1. Si reduces hardenability because it tends to promote pearlite formation in some martensitic irons.[2]
2. However, in the presence of pearlitic-suppressing elements such as Mo, Ni, Mn, and Cr, increased Si has been found to increase the amount of martensite and resulting hardness in other high-alloy white cast irons.[2,3]

3. Silicon reduces carbon solubility in austenite and hence the hardness of heat-treated HCWI castings.
4. A general reference[2] and ThermoCalc© analysis indicate that Si lowers the eutectic carbon content.

Numerous articles have been published describing the metallurgy of the HCWI irons.[4-11] Despite what is known about Si, little research[10,11] has been conducted to quantify the effects of Si in High-Cr white irons.

BACKGROUND INFORMATION

ASTM specification A532 covers the compositions and minimum required hardness values of two general classes of the high-chromium irons.[1] The chromium-molybdenum irons (Class II of ASTM A532) contain 11 to 23% Cr and up to 3.5% Mo. Class II alloys and can be supplied in either the as-cast condition with an austenitic or austenitic-martensitic matrix, or in the heat-treated condition with a martensitic matrix microstructure.
The high-chromium irons (Class III of ASTM A532) represent the oldest grade of high-chromium irons, with the earliest patents dating back to 1917. These general-purpose irons, also called 25% Cr and 28% Cr irons, contain 23% to 28% Cr with up to 1.5% Mo. To prevent pearlite and attain maximum hardness, molybdenum is added in all but the lightest-cast sections. Although the maximum attainable hardness is not as high as in the Class II chromium-molybdenum white irons, these Class III alloys are often selected for heavy section castings and when resistance to corrosion is also desired.

Most HCWI castings are heat-treated for maximum hardness, abrasion resistance and toughness. They are generally considered the hardest of all grades of white cast irons. Compared to the lower-alloy Ni-Cr white irons (Class I), the eutectic carbides are harder and the matrix can be heat treated to achieve castings of high hardness (>700 HB). Molybdenum, as well as nickel and copper when needed, is added to prevent pearlite and ensure maximum hardness.

During eutectic solidification, Si is rejected by the carbides and partitions to the metallic (austenite) phase, producing higher Si concentrations in the metallic matrix. Cias[12] reported that Si reduces hardenability in HCWI castings, as shown in the continuous cooling transformation (CCT) diagram in Figure 1.

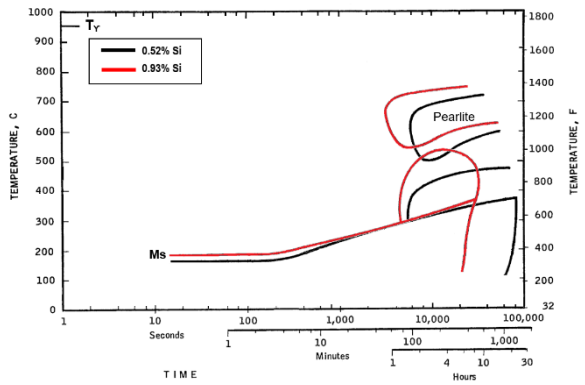

Figure 1. CCT diagrams for two 18%Cr white irons containing 0.52% and 0.93% Si.[10] T_Y and M_S are austenitizing and martensite-start temperatures, respectively.

The reason for the negative coefficient for Si in many hardenability calculations may be due to its negative effect on C solubility. However, Si has been shown to enhance hardenability in medium-carbon steels, e.g., as in 4340 (300M) and in the Climax Molybdenum Co. medium-carbon Cromosil steels.[13] The Si also weakly enhances hardenability in low-alloy steels.

Possibly at the optimum hardening temperature, Si can partially supplant the more expensive alloying elements (Mo, Cu and Ni) that are typically added to Class II HCWI for hardenability. If so, an adjustment (an increase) in the hardening temperature may restore hardenability in HCWI irons with higher Si concentrations.

It is also possible that high Si concentrations might prove beneficial in the heat treatment of Class II alloys (Cr-Mo irons). Since the optimum hardening temperature [<1700F (925C)] for 15% Cr irons is too low for direct hardening, an elevated Si concentration could raise the optimum hardening temperature to a more practical hardening temperature [≥1750F (955C)] where austenite destabilization can occur in shorter and more practical holding times.

TECHNICAL APPROACH AND INNOVATION

This study intended to define the various influences that silicon has on the microstructure and heat treatment response of high-Cr white cast irons. Alloys of both ASTM A532 Class II and Class III were studied.
Solution heat treatment at a series of temperatures between 1600 and 2000 F (872 and 1090 C) were employed to help determine the optimum hardening temperature in each class of alloys. The results were used to characterize the effect of Si on the optimum hardening temperature in HCWI. Heat treatment experiments at various cooling rates were used to determine the position of the pearlite nose.

The investigators employed chemical analysis, thermal analysis and determination of eutectic carbide fraction by image analysis to determine the effects of Si on eutectic saturation. The results were intended to show the influence of Si on hardenability in HCWI alloys.

EXPERIMENTAL PROCEDURES & RESULTS

ALLOY DESIGN AND CASTING

The experimental work focused on Class II and Class III alloys of ASTM A532, with the aim chemistries listed in Table 1.

Table 1. Aim Compositions for Six Experimental Alloys, wt %

Heat	1	2
C	3	2.6
Cr	15	25
Mn	0.7	0.7
Mo	0.5	Residual
Ni	0.75	Residual
Cu	0.75	Residual
Si	0.4, 1.0 and 1.6	0.4, 1.0 and 1.6

For this study, 1000 lb. (450 kg) master heats were produced in a commercial foundry. The C and Cr levels were fixed for each base iron alloy. The Si content was increased incrementally in the furnace to obtain alloys at three Si concentrations (nominally 0.4%, 1% and 1.6%).The charge materials consisted of pig iron, steel scrap, graphite, FeCr, FeSi, FeMn, FeMo, Cu wire and Ni plate. The molten metal processing consisted of superheating to 2750F (1510C) and holding while chemistry was adjusted, followed by cooling to and holding at 2650F (1455C).

Each tap consisted of transferring 250 lbs. (113 kg) to the pouring ladle. Two 3-inch (75-mm) Y-block castings were poured from the ladle. At the same time, FeSi and FeCr additions were made to the furnace to adjust melt chemistry to the desired Si level. The pouring temperatures ranged from 2450 to 2550F (1110 to 1155C). Table 2 lists the final compositions for the six HCWI alloys.

Table 2. Chemical Compositions of Experimental Alloys, wt %

Element	Heat 1 – 15%Cr series			Heat 2 – 25%Cr series			*Method**
	A	**B**	**C**	**A**	**B**	**C**	
C	2.98	3.11	2.94	2.50	2.58	2.54	*L*
S	0.020	0.022	0.019	0.027	0.025	0.028	*L*
P	0.012	-	-	0.012	-	-	*OES*
Si	0.41	-	-	0.44	-	-	*OES*
Si	0.44	0.98	1.62	0.46	0.99	1.56	*ICP*
Mn	0.66	-	-	0.61	-	-	*OES*
Cr	14.69	-	-	24.85	-	-	*OES*
Cr	14.71	14.57	14.85	24.76	25.10	24.78	*ICP*
Cu	0.71	-	-	0.05	-	-	*OES*
Ni	0.73	-	-	0.14	-	-	*OES*
Mo	0.64	-	-	0.04	-	-	*OES*
V	0.028	-	-	0.045	-	-	*OES*
Al	<0.008	-	-	<0.008	-	-	*OES*
Ti	<0.008	-	-	<0.008	-	-	*OES*
Sn	<0.008			<0.008			*OES*
Fe	Base			Base			

*L = Leco combustion method (ASTM E1019)
ICP = Inductively-coupled Plasma (ICP) Spectroscopy
OES = Optical Emission Spectroscopy

Thermal analysis cups were also poured from each split heat. Figure 2 illustrates the typical cooling curve for the thermal analysis cups.

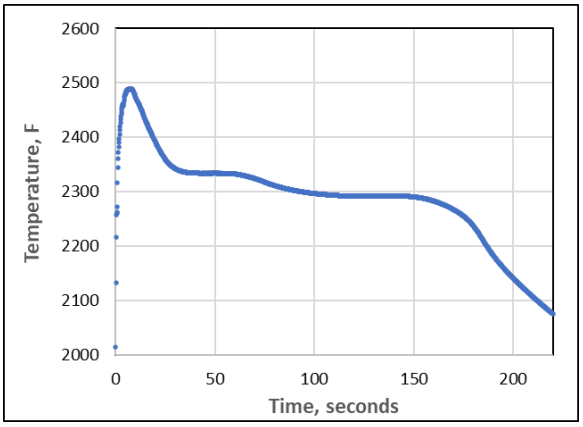

Figure 2. Cooling curve for the thermal analysis cup of the 25%Cr-1Si HCWI alloy.

Table 3 lists the inflection points of the thermal analysis time-temperature curves for five of the alloys.

Table 3. Thermal Arrest Temperatures from Thermal Analysis Cups

Alloy	Nominal Composition	$T_{liquidus}$, F	$T_{solidus}$, F	ΔT, F
1A	3.0C-15Cr-0.4Si	2304	2221	83
1B	3.1C-15Cr-1.0Si	2280	2215	65
1C	2.9C-15Cr-1.6Si	2283	2218	65
2B	2.6C-25Cr-1.0Si	2337	2299	38
2C	2.5C-25Cr-1.6Si	2334	2292	42

The Y-block castings poured for this study generally conformed to the 3-inch (75-mm) standard Y-block design of ASTM A536 specification, but the ASTM Y-block was extended to 7.5 inches (190 mm) in length. A schematic of the modified Y-block casting is shown in Figure 3. For general information, the section modulus of the casting (SA/V ratio) is 1.213 per inch, which is equivalent to a 3.3-inch (85-mm) round or a 1.65-inch (40-mm) plate casting.

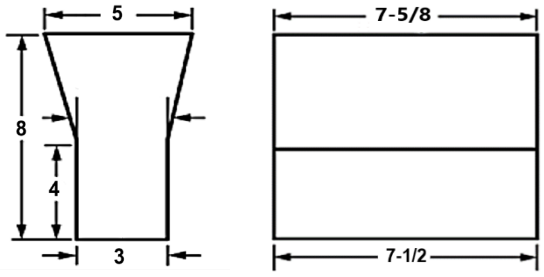

Figure 3. Modified 3-inch Y-block used in experimental HCWI iron heats. All dimensions are in inches.

SAMPLE PREPARATION

The Y-blocks were sectioned on a water-jet saw to obtain various samples for testing and experimental heat treatments. Initially, a 1 x 3 x 7.5-inch (25 x 75 x 190-mm) long slab was removed from the bottom of each Y-block leg. All slabs of the six alloys were then subcritically annealed at 1112F (600C) for 8 hours. The slab was sectioned further using wire-electrical-discharge machining (EDM) to produce numerous small samples measuring 1 x 1 x 1 inch (25 x 25 x 25 mm).

Initially, experimental heat treatments were conducted to determine the heat treatment response at different austenitizing temperatures. The small samples were used to determine the optimum heat treatment temperature for each alloy. Subsequently, additional samples were sectioned and heat treated to determine the kinetics of pearlite transformation.

Samples were also cut from the slab for determining the volume fraction of eutectic carbides and the distribution of the primary alloying elements in the as-cast microstructure. The evaluated surface was located 1 inch (25 mm) above the bottom cast face, 1 inch (25 mm) in from the side face, and at least 1 inch (25 mm) from the end face of the Y-block leg.

ANNEALED MICROSTRUCTURES

Metallographic specimens were obtained from each alloy and the specimens were compression-mounted in Bakelite and then ground, polished, and etched in accordance with ASTM E3. (All metallographic mounts were similarly prepared in this study.) After polishing, the as-cast and annealed samples were etched in 4% Nital.

Low magnification examinations (Figures 4 and 5) show that all the alloys appear similar, although the three alloys with higher Cr contents may have slightly refined microstructures.

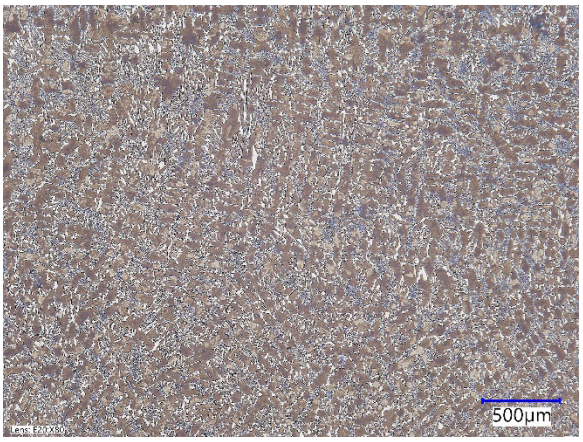

(a) Alloy 1A, Original Magnification (OM) = 25x

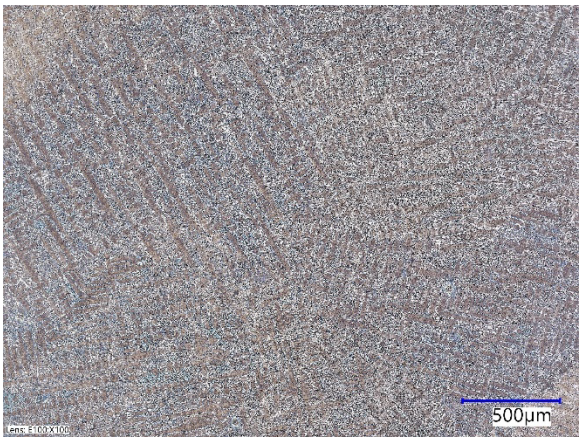

(a) Alloy 2A, OM = 30x

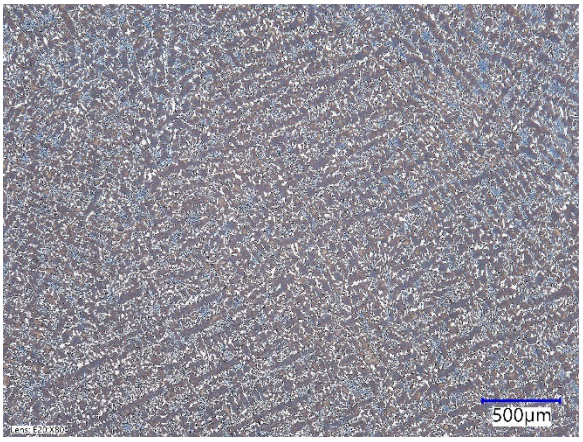

(b) Alloy 1B, OM = 25x

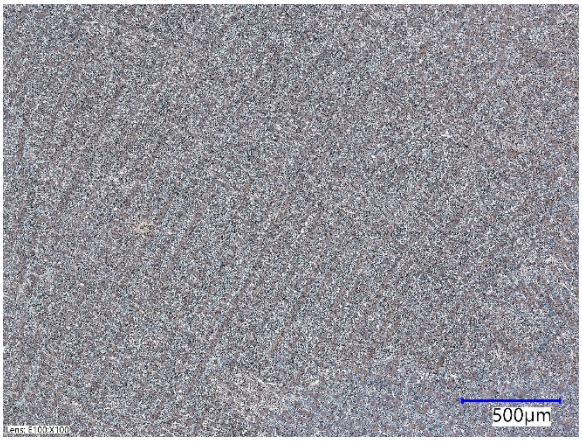

(b) Alloy 2B, OM = 30x

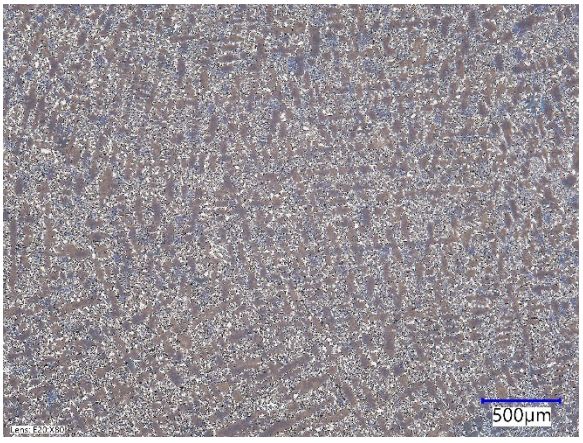

(c) Alloy 1C, OM = 30x

Figure 4. Annealed microstructures of Alloys 1A through 1C (Views a-c) at low magnification after etching in 4% Nital.

(c) Alloy 2C, OM = 30x

Figure 5. Annealed microstructures of Alloys 2A through 2C (Views a-c) at low magnification after etching in 4% Nital.

At higher magnification, Figure 6 shows that the leanest alloy exemplifies the mixture of pearlite, intergranular hypereutectic chromium carbide, and finer eutectic carbide clusters. All the alloys had similar constituents.

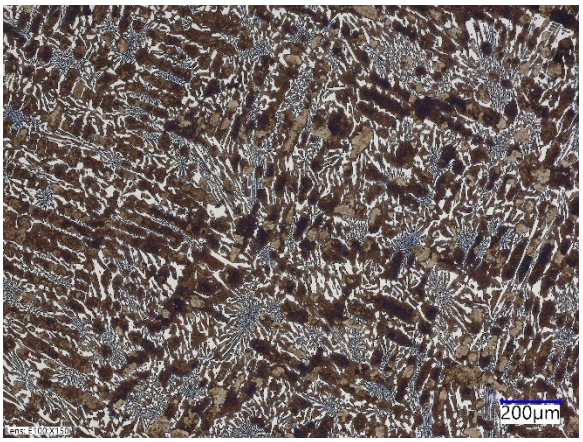

(a) OM = 50x

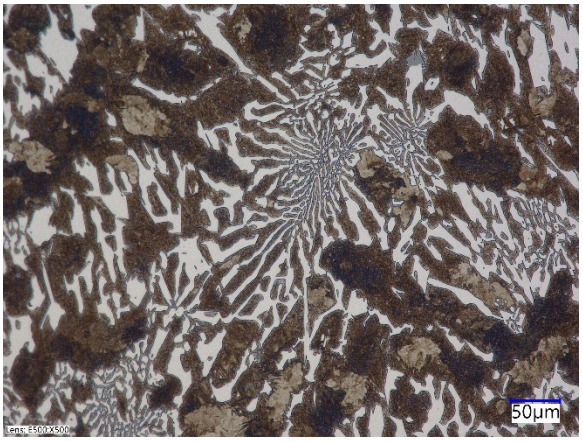

(b) OM = 175x

Figure 6. Annealed microstructures of Alloy 1A at higher magnifications after etching in 4% Nital.

The alloys were then etched with a permanganate solution containing 4g $KMnO_4$ + 4g NaOH in 100 ml distilled water. This solution stain-etched the metallic matrix, leaving the eutectic carbides un-etched and sufficiently distinguished the matrix from the carbides. Automated optical image analysis (IA) was performed on 80 fields with individual field size of 0.19 mm^2 for a total analyzed area of 15 mm^2.

The mean area-percent carbide was determined by image analysis and the results are listed in Table 4.

Table 4. Carbide Fraction in Six HCWI Alloys

Alloy	Nominal Composition	% Carbide
1A	3.0C-15Cr-0.4Si	31.1
1B	3.1C-15Cr-1.0Si	32.2
1C	2.9C-15Cr-1.6Si	31.6
2A	2.5C-25Cr-0.4Si	29.0
2B	2.6C-25Cr-1.0Si	27.7
2C	2.5C-25Cr-1.6Si	24.4

ENERGY DISPERSIVE SPECTROSCOPY

Scanning electron microscopy and energy dispersive spectrometry (SEM/EDS) were used to investigate the distribution of the solute elements in the six HCWI alloys. The same metallographic samples used to determine carbide fraction were used for SEM/EDS analysis.

The specimens were placed in an SEM, and two to three locations for each of three constituents were probed for elemental content, including the eutectic carbides, the primary austenite dendrites and the eutectic metallic matrix located within the radial eutectic carbides. Figure 7 illustrates the typical field with the three types of microconstituents that were analyzed.

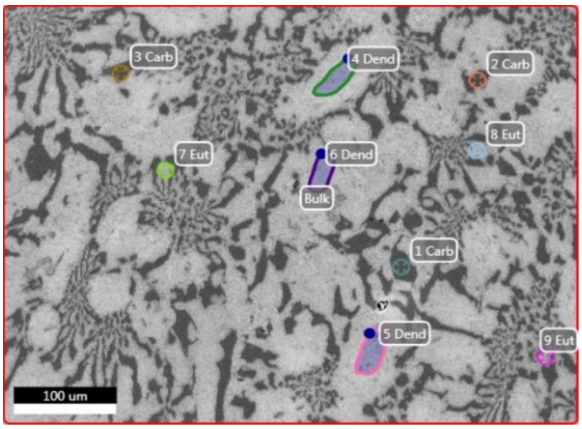

Figure 7. Electron micrograph of a field used to determine elemental distributions by SEM/EDS spectrometry in a 25%Cr HCWI alloy. "Dend" = primary austenite dendrite, "Carb" = eutectic carbides, and "Eut" = eutectic matrix.

Table 5 summarizes the average elemental contents for each of the three constituents in each alloy

Table 5. Results of Semiquantitative EDS Analysis of Elemental Distributions in HCWI Alloys, wt%

Constituents	C	Si	Cr	Mo	Mn	Ni	Cu	Fe
Alloy 1A—Low Cr with Low Si								
Carbide	9.5	0.13	45	0.57	0.95	0.20	0.14	43
Dendrite	5.1	0.36	11	0.24	0.91	1.26	1.3	80
Eutectic Matrix	4.0	0.31	8.4	0.20	0.77	1.20	1.1	84
Alloy 1B—Low Cr with Intermediate Si								
Carbide	9.5	0.13	46	0.71	1.3	0.30	0.32	45
Dendrite	4.2	0.82	9.5	0.16	0.7	1.1	1.1	83
Eutectic Matrix	4.8	1.0	7.3	0.18	0.9	1.3	1.4	83
Alloy 1C—Low Cr with High Si								
Carbide	9.5	0.05	45	0.57	1.1	0.26	0.22	43
Dendrite	4.7	1.3	10	0.13	0.60	0.95	1.1	81
Eutectic Matrix	4.4	1.6	7.2	0.27	0.87	1.23	0.95	83
Alloy 2A—High Cr with Low Si								
Carbide	9.8	0.13	59	0.25	1.3	0.28	0.23	29
Dendrite	4.1	0.33	18	0.07	0.91	0.41	0.25	76
Eutectic Matrix	3.5	0.36	17	0.05	0.88	0.37	0.30	77
Alloy 2B—High Cr with Intermediate Si								
Carbide	9.9	0.03	60	0.08	0.88	0.32	0.29	29
Dendrite	3.6	0.71	18	0.02	0.85	0.47	0.41	76
Eutectic Matrix	4.2	0.57	17	0.02	0.99	0.35	0.32	64
Alloy 2C—High Cr with High Si								
Carbide	9.8	0.04	60	0.05	1.2	0.26	0.23	29
Dendrite	4.2	1.3	18	0.12	1.1	0.48	0.44	75
Eutectic Matrix	3.8	1.5	15	0.11	1.0	0.49	0.37	78

EXPERIMENTAL HEAT TREATMENTS

The optimum hardening temperature for each alloy was determined. Each sample was coated with Condursal Z1100®, a proprietary protective paint, to prevent excessive scaling and decarburization. The samples were then placed in stainless steel foil envelopes to further protect them from oxidation during heat treatment in a laboratory, resistance-heated box oven. The heating cycle consisted of slow-heating in two stages through the pearlite transformation region followed by further heating to various austenitizing temperatures (T_A) ranging from 1600 to 2000F (871 to 1093C) in 40°F (22°C) intervals. The samples were held at the austenitizing temperature for 2 hours and then quenched in air to room temperature, while the samples were still contained in the protective SS envelopes.

The following steps summarize the heat treatment cycle:

- Heat to 1200F (649C) and hold 1h,
- Heat at 30°F/h (17°C/h) from 1200 to 1350F (649 to 732C),
- Heat to T_A at 200°F (111°C)/h,
- Soak at T_A for 2h,
- Air Quench

HARDNESS TESTING

After the heat treatments were completed, the test samples were ground to remove the oxidized and decarburized layers at the surface of the sample. The EDM surface of the samples was ground flat through 180-mesh abrasive papers. Brinell hardness was determined in triplicate using a 10-mm diameter tungsten carbide indenter and 3000-kg load. The testing was conducted in accordance with ASTM E10. The Brinell indentations were measured on a metallograph with software for determining the mean diameter of the impression. Each impression was measured to the nearest 0.001 mm.

The average Brinell hardness is plotted against austenitizing temperature in Figure 8.

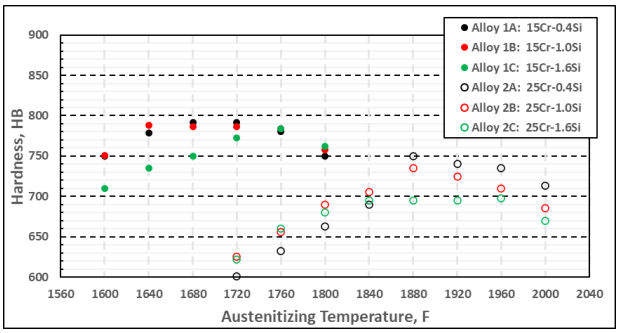

Figure 8. Hardness versus hardening temperatures for the 15% and 25%Cr HCWI alloys.

TRANSFORMATION KINETICS

Additional test samples were used in heat treatment studies to determine the position of the pearlite nose on cooling from the optimum austenitizing/hardening temperature. Once again, the test samples were removed from the 1-inch slab that had been removed from the bottom of each Y-block as described above in the Sample Preparation section. The samples were placed in stainless steel foil envelopes to protect them from oxidation and scaling.

The samples were placed in a laboratory, resistance-heated, box furnace and heated to the desired hardening temperature for each alloy. Based on Figure 8, the three 15% Cr alloy samples were heated for 4 hours to 1760F (960C), which was the optimum hardening temperature of the 1.6% Si variant of the 15% Cr series. Likewise, for the three 25% Cr alloys, the samples were heated for 2 hours to 1920F (1049C), which was the optimum hardening temperature of the 1.6% Si variant of the 25%Cr series. Following heating at the desired austenitizing temperature, the samples were cooled at various rates, i.e., the rates predicted to cross the pearlite nose on cooling.

The fastest cooling rates consisted of furnace cooling in two laboratory ovens of different sizes, which produced natural cooling. Additional heat treatments were conducted at slower rates by controlled cooling using a programmable temperature controller. Three cooling rates were applied for each Cr series. The goal of these heat treatments was to determine the critical cooling rate to intersect the pearlite nose in continuous cooling. Representative cooling curves for the various cooling conditions are shown in Figure 9.

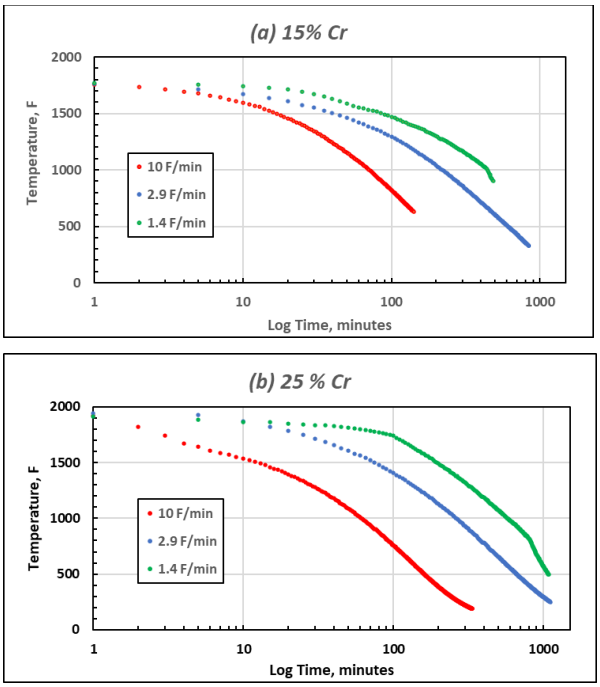

Figure 9. Cooling curves of test samples of (a) 15%Cr and (b) 25%Cr alloys heated at, and cooled from 1760 and 1920F (960 and 1049C), respectively.

Following the experimental heat treatments, metallographic mounts were prepared as described previously and etched in 2% Nital. The area-percent pearlite was estimated for each sample by manual point counting and the results are listed in Table 6.

Table 6. Results of the Transformation Study

Alloy	Nominal Composition	Pearlite Content, %		
		Cooling Rate 1, 10 F/min (5.5 C/min)*	Cooling Rate 2, 2.9 F/min (1.6 C/min)	Cooling Rate 3, 1.4 F/min (0.8 C/min)
1A	15Cr-0.4Si	2-3%	10-15%	90%
1B	15Cr-1.0Si	10-15%	40%	98%
1C	15Cr-1.6Si	15-20%	60-70%	100%
2A	25Cr-0.4Si	0%	25%	-
2B	25Cr-1.0Si	0%	10-15%	-
2C	25Cr-1.6Si	0%	1-2%	-

*Average cooling rate between 1400 and 1200 F (760 and 650 C)

Since pearlite transformation is generally completed before reaching 1200F (650C) in HCWI alloys, the cooling rate between 1500 and 1200F (816 and 650C) was used as a gage for estimating the critical cooling rate to avoid pearlite formation. The average results from Table 6 are plotted in Figure 10 to illustrate the influence of Si on the position of the pearlite nose for the 15% Cr alloy series.

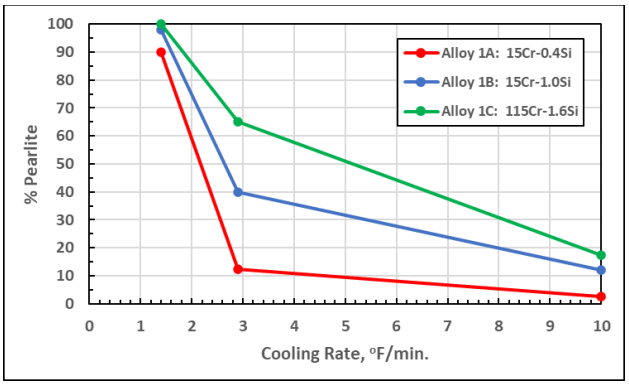

Figure 10. Effect of cooling rate on % pearlite formed in samples of the 15% alloys heated to and cooled from 1760F (960C).

DISCUSSION

STUDY OBJECTIVES

The principal objectives of this investigation were to determine the effects of Si on (1) the peak austenitizing temperature, (2) the hardenability, and (3) the shift in % carbon at eutectic saturation in hypoeutectic 15% and 25% Cr white irons. Three levels of Si were studied in each alloy.

The successful heat treatment of HCWI castings will produce austenite "destabilization", i.e., raise the Ms temperature well above room temperature, by the precipitation of fine and secondary M_7C_3 carbides within the austenite matrix. Carbide precipitation reduces the dissolved carbon content and allows the austenite to reach equilibrium carbon concentrations at the austenitizing temperature. The concentration of the carbon dissolved in the austenite generally increases with temperature.

HARDENING COMPARISONS

There is an optimum austenitizing temperature for achieving maximum hardness. The austenitizing temperature controls the amount of carbon that remains in solution, and low temperatures result in low-carbon austenite, which produces low-carbon martensite with reduced hardness. As temperature increases, carbon solubility increases and hardness of the martensite matrix also increases. At some point, carbon solubility is excessive, the Ms temperature is depressed, and the austenite phase becomes more stable, which promotes decreased hardness due to elevated levels of retained austenite. At the optimum temperature, maximum hardness is obtained. The influence of austenitizing temperature on retained austenite and hardness are depicted in Figure 11.

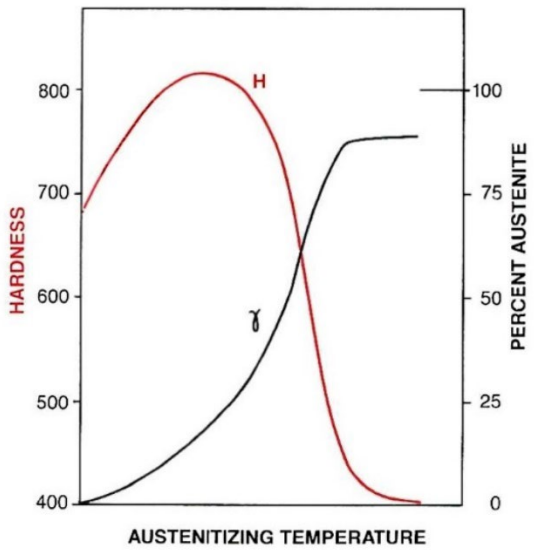

Figure 11. Influence of austenitizing temperature on hardness (H) and retained austenite (γ) in high-chromium irons[6,15]

The optimum hardening temperature varies with composition, particularly with C and Cr contents, which in turn, control austenite carbon solubility. As the bulk Cr level in HCWI alloys increases, the carbon solubility in austenite decreases, and the temperature of peak hardness must increase. Figure 8 shows that the optimum hardening temperature was substantially higher in the 25% Cr series [1920F (1050C)] compared to the 15% Cr series [1680F (915C)].

The silicon has a significant effect on austenite carbon solubility in the graphitic irons, and it was anticipated that Si would cause a shift in the optimum hardening temperature in HCWI alloys. Indeed, as Si increased, the temperature of peak hardness also increased in the 15% Cr series. For this series, the peak hardening temperature was raised 80F (44C) from 1680 to 1760F (915 to 960C) for an increase of 1.2%Si, that is, when Si increases from 0.4 to 1.6%. However, with a comparable increase in Si (1.1%Si), the peak hardening temperature [1920F (1050C)] for the 25% Cr series was unchanged.

It is also noteworthy that peak hardness was significantly higher in the leaner Cr alloys and the peak hardness decreased slightly with increasing Si content. In the 15% Cr series, peak hardness dropped from 790 HB to 770 HB for Si levels of 0.4% and 1.6%, respectively. In the 25% Cr series, peak hardness dropped from 740HB to 720 HB for Si levels of 0.4 and 1.6%, respectively.

It should be noted that the optimum hardening temperature for the base 15% Cr alloy is rather low. Destabilization times at 1680F (915C) can be quite long (>8h), due to the slow diffusion rate of Cr to the growing carbide phase at this temperature. However, Maratray[8] has shown that, when the starting structure is pearlitic, destabilization times are greatly reduced. For this study, heating was slowed during heating through the pearlite nose [1300F (705C)] in order to convert any retained austenite to pearlite prior to heating to the destabilization temperature.

HARDENABILITY

The experiments with varying cooling rates were quite revealing. The critical rates to produce pearlite are shown in Table 6 and Figure 10. In the 15%Cr series, Si reduced hardenability, that is, it raised the critical rate at which the first pearlite was observed. The decrease in hardenability is consistent with the CCT study reported by Cias[12] for 18% Cr HCWI alloys and as shown in Figure 1.

In contrast, for the 25% Cr series, the test results were quite the opposite. Table 6 shows that Si delayed pearlite transformation to longer times and increased the hardenability of the 25% Cr series. This result is consistent with the hardenability effect observed for Si in steels.[13,14]

Si & EUTECTIC SATURATION

Despite the fact that ThermoCalc© calculations predicted a significant increase in eutectic saturation or “carbon equivalent” in HCWI alloys, the thermal analysis records indicated that Si had no significant effect on reducing the temperature difference between austenite liquidus and the solidus temperatures, see Table 3. Likewise, when the minor variations in C and Cr contents of the experimental alloys were considered, the results of image analysis in Table 4 showed no consistent increase in eutectic carbide fraction with increasing Si. In fact, the fraction of eutectic carbide decreased with increasing Si in the 25% Cr series.

DISTRIBUTION OF ALLOYING ELEMENTS

The results of SEM/EDS analysis are presented in Table 5. It must be emphasized that EDS is a semiquantitative technique that is well-known to yield only comparative analyses for carbon. Therefore, the carbon contents in Table 5 cannot be directly compared to the accurate carbon contents reported in Table 2. However, the carbon contents can be compared qualitatively, between alloys and constituents, within Table 5. Furthermore, EDS analysis of tiny microstructural features is also limited by the X-ray generation volume exceeding the volume of the feature being analyzed.

The EDS findings were predictable in that much of the Cr partitioned to the eutectic carbides during solidification. The carbides were much richer in Cr than that in the bulk composition (Table 2). The Cr content of the carbides in the 15% Cr series averaged 44%, and averaged 60% in the 25% Cr series. Si additions did not appear to affect the %Cr in the eutectic carbides.

In contrast, the Cr content of the primary dendrites was significantly lower than that of the bulk alloy with an average of 10.1% Cr in the 15% Cr series and 18% Cr in the 25% Cr series. The Si additions did not appear to affect the % Cr in the primary dendrites.

The eutectic matrix contained the lowest Cr contents, with an average of 7.6% Cr in the 15% Cr series and 16.5% Cr in the 25% Cr series.

For both the 15% Cr and 25% Cr series, the Mn and Mo concentrations were elevated in the eutectic carbides. In contrast, Ni and Cu were quite low in the eutectic carbides.

Little Si was detected in the eutectic carbides. However, the Si concentrations in the primary dendrites and eutectic matrix generally reflected that of the bulk chemistry.

CONCLUSIONS

This research characterized the effects of Si on the optimum hardening temperature, hardenability, and eutectic saturation in hypoeutectic high-Cr white cast irons in 3-inch (75 mm) Y-blocks containing 15% and 25%Cr. Hypoeutectic alloys of 15% and 25% Cr white irons were produced with Si levels varying from 0.4%, 1% and 1.6% Si when poured.

1. Raising Cr from 15% to 25% caused the optimum hardening temperature to rise from 1680 to 1920F (915 to 1050C).

2. The effects of Si on hardening temperature varied with Cr content. In the 15% Cr series, an increase of 1.2% Si raised the optimum hardening temperature by 80°F (44°C). For the 25% Cr series, the optimum hardening temperature was unchanged.

3. Peak hardness was significantly higher in the leaner Cr alloys and the peak hardness decreased slightly with increasing Si content. In the 15% Cr

series, peak hardness dropped from 790 HB to 770 HB for Si levels of 0.4% and 1.6%, respectively. In the 25% Cr series, peak hardness dropped from 740HB to 720 HB for Si levels of 0.4 and 1.6%, respectively.

4. The effect of Si on hardenability was mixed. Si reduced the hardenability in the 15% Cr series. However, Si raised the hardenability in the 25% Cr series.

5. The influence of Si on % eutectic saturation was not clear. Thermal analysis indicated that Si raised eutectic saturation modestly, whereas in the 25% Cr series, the effect of Si on eutectic saturation was not significant. When analyzing carbide fraction, Si had a negligible effect in the 15% Cr series, but seemed to cause the 25% Cr series to develop less eutectic carbide, that is, become more hypoeutectic.

6. SEM/EDS analysis was conducted to determine the distributions of Si, Cr, Mn, Ni, Mo, and Cu among the various solidification constituents, including the primary austenite dendrites, eutectic austenite and the eutectic carbides. Cr was richest in the eutectic carbides and leanest in the eutectic austenite matrix. The Si was largely rejected from the eutectic carbides and richest in the eutectic austenite.

ACKNOWLEDGEMENTS

The authors acknowledge funding from the American Foundry Society under Memorandum of Agreement (MOA) 22-23 #3. The authors thank Alliant Castings of Winona, Minnesota for supplying the white iron castings. Furthermore, the authors are grateful for the guidance that they received from the AFS monitoring committee composed of the following AFS Special Irons Committee members: Perry Kamrowski (Alliant Castings, Chair), David Havel (Columbia Steel Cast Products, LLC), Brian Bendig (Penticton Foundry), John Cory (Magotteaux), and Jerrod Miller (Wear-Tek).

REFERENCES

1. “Standard Specification for Abrasion-Resistant Cast Irons,” ASTM A532/532M-10 (Reapproved 2019), ASTM International (2019).
2. Richard B. Gundlach and Douglas V. Doane, “Alloy Cast Irons,” in “Properties and Selection: Irons, Steels, and High-Performance Alloys,” ASM Handbook, Vol. 1, pp. 85-104 (1990).
3. J.R. Keough and K.L. Hayrynen, “Heat Treatment of High-Alloy White Cast Irons,” “Cast Iron Science and Technology,” ed. D.M. Stefanescu, ASM Handbook, Vol. 1A, pp. 275-283 (2017).
4. J. Dodd, and J.L. Parks, “Factors Affecting the Production and Performance of Thick Section High Chromium-Molybdenum Alloy Iron Castings” Climax Molybdenum Company, Metals Forum (1980).
5. W. Fairhurst and K. Rohrig, “Abrasion-resistant high-chromium white cast irons,” *Foundry Trade Journal* (1974).
6. Richard B. Gundlach, “White Iron and High-Alloyed Iron Castings” in “Casting,” ASM Handbook, Vol. 15, pp. 896-903 (2008).
7. F. Maratray, “Choice of Appropriate Compositions for Chromium-Molybdenum White Irons,” *AFS Transactions*, v.79, p. 121-124 (1971).
8. F. Maratray, and R. Usseglio-Nanot, “Factors Affecting the Structure of Chromium and Chromium-Molybdenum White Irons,” publ. Climax Molybdenum Company (circa 1970).
9. “Abrasion-Resistant Cast Iron Handbook,” ed. G. Laird, R. Gundlach and K. Rohrig, American Foundry Society (2000).
10. Jian-Ping Lai, Qing-Lin Pan, Yuan-Wei Sun and Chang-An Xia, “Effect of Si Content on the Microstructure and Wear Resistance of High Chromium Cast Iron,” *ISIJ International,* Vol. 58, No. 8, pp. 1532–1537 (2018).
11. Ying-long Su, Dan Li, and Xue-kun Zhang, “Optimizing Hardenability of High Chromium white cast iron,” *China Foundry* (Nov. 2006.)
12. W.W. Cias, “Austenite Transformation Kinetics of Ferrous Alloys, Vol. II: Cast Irons and Steels,” Climax Molybdenum Company, pp. II-52 and II-53 (circa 1980).
13. “CrMoSil Steels,” Climax Molybdenum Company (circa 1980).
14. J.M. Tartaglia and G.T. Eldis, “Core Hardenability Calculations for Carburizing Steels,” *Metallurgical Transactions A,* Vol. 15A, pp. 1173-1183 (June 1984).
15. “Chrome-Moly White Cast Irons,” AMAX publication, M-630 (2/86).